63-3-2

SSD-TDR-63-27

REPORT NO.
TDR-169(3240-11)TN-2

Yielding and Flow of Iron

27 FEBRUARY 1963

Prepared by HANS CONRAD
Materials Sciences Laboratory

Prepared for COMMANDER SPACE SYSTEMS DIVISION
UNITED STATES AIR FORCE
Inglewood, California

LABORATORIES DIVISION • AEROSPACE CORPORATION
CONTRACT NO. AF 04(695)-169

SSD-TDR-63-27

Report No.
TDR-169(3240-11)TN-2

YIELDING AND FLOW OF IRON

Prepared by

Hans Conrad
Materials Sciences Laboratory

AEROSPACE CORPORATION
El Segundo, California

Contract No. AF 04(695)-169

27 February 1963

Prepared for

COMMANDER SPACE SYSTEMS DIVISION
UNITED STATES AIR FORCE
Inglewood, California

ABSTRACT

The significance of the parameters of the Hall-Petch equation

$$\sigma = \sigma^*(T, \dot{\epsilon}) + \sigma_\mu(st) + kd^{-1/2}$$

for yielding and flow of iron and steel are discussed. The available experimental data suggest that σ^* represents the thermally-activated overcoming of the Peierls-Nabarro stress. The variations in σ^* with structure can be interpreted as changes in either dislocation density contributing to the deformation or the average distance the dislocations move per successful thermal fluctuation. Good agreement between experiment and theory is found for the contributions to σ_μ of interstitials in solution, precipitate particles, and strain. The significance of k is still unresolved.

The experimental data suggest that the yield point in iron and steel is not due to the thermally-activated unlocking of dislocations from an interstitial atmosphere, but rather is associated with the decrease in dislocation velocity due to the sudden multiplication of dislocations by the double cross-slip mechanism. Stress-strain curves for mild steel calculated on the basis of this latter mechanism are in good agreement with the experimental curves.

ACKNOWLEDGEMENT

I would like to express appreciation to P. Haasen and A. S. Keh for permission to use some of their experimental results prior to publication.

CONTENTS

FIGURES

I. INTRODUCTION

The present discussion covers yielding and flow of iron from a different viewpoint than that of Allen (Ref. 1) or Low (Ref. 2). Special attention is here given to the identification of the dislocation mechanisms responsible for the parameters of the Hall-Petch equation (Refs. 3 - 5). Also, an explanation for the yield point is given, which appears to be in better agreement with the experimental data than Cottrell's theory (Ref. 6) of breaking away from an interstitial atmosphere. This discussion will only be concerned with iron and steel where the effects of alloying elements other than the interstitials are negligible.

II. HALL-PETCH EQUATION FOR YIELDING AND FLOW

Considerable experimental data indicate that the yield stress and flow stress in iron and steel obey the relation (Refs. 3-5 and 7-9)

$$\sigma = \sigma^*(T, \dot{\epsilon}) + \sigma_\mu(st) + kd^{-1/2} \qquad (1)$$

σ^* is the thermal component of the stress that may depend on composition (Ref. 8), strain (Refs. 10 and 11), and whether the specimen is single or polycrystalline (Ref. 8), as well as on the temperature T and the strain rate $\dot{\epsilon}$. σ_μ is the athermal component of the stress that is related to the structure associated with dislocations, C + N in solution, precipitates, etc., (Refs. 12 and 13) and is proportional to the shear modulus μ. k is the slope of the straight line obtained when the yield or flow stress is plotted versus the reciprocal of the square root of the grain size d and is relatively independent of temperature and strain rate over the range 100°-300°K (Refs. 7, 14, and 15), but may depend on composition (Ref. 15). The value of k for flow is approximately equal to that for yielding (Refs. 9 and 16).

The effect of C and N content on σ^* is most pronounced for concentrations below about 0.01 wt% (Ref. 8) (see also Fig. 12 in Ref. 1). Similarly, the effect of interstitials on k is most marked at very low concentrations. Furthermore, N has a greater effect on k than does C (Ref. 13). In regard to the effect of interstitials on σ_μ, Heslop and Petch (Ref. 13) have shown that σ_μ increases in a linear manner with the amount of C + N in solution; also, σ_μ depends on the presence and dispersion of interstitial precipitates.

A decrease in σ^* with strain has been observed for decarburized Ferrovac iron (Ref. 10) and for vacuum-melted electrolytic iron (0.014 percent C) quenched from 920°C (Ref. 11). On the other hand, an increase in σ^* with

strain over the temperature range 200°-300°K has been observed for single crystals made from Carbonyl iron (Ref. 17). Essentially no effect of strain on σ^* occurred for annealed vacuum-melted electrolytic iron (Ref. 7) or annealed Ferrovac ion (Ref. 10).

The increase of σ_μ with strain in polycrystals (i.e., the strain hardening coefficient decreases with strain) is of the order of $5 \times 10^{-3}\mu$ at a strain of 0.1 and is relatively independent of temperature and grain size (Ref. 18).

The effect of grain size on σ^* becomes noticeable only at very large grain sizes, for example, when comparing single and polycrystalline specimens (Ref. 8). (Also see Fig. 17 in Ref. 2.)

The interpretation of the parameters of Eq. 1 and their variation with interstitial content, strain, grain size, etc., will now be discussed.

III. INTERPRETATION OF σ^*

It is now generally accepted that the deformation of metals may be thermally activated; if a single mechanism is rate-controlling, one can write

$$\dot{\gamma} = \rho bv = \rho bs\nu^* \exp\left\{-\frac{H(\tau, T)}{kT}\right\} \tag{2}$$

for the shear strain rate $\dot{\gamma}$, where ρ is the density of dislocations contributing to the deformation, b is the Burgers vector, v is the average velocity of the dislocations, s is the average distance a dislocation moves after each successful thermal fluctuation, ν^* is the frequency of vibration of the dislocation segment involved in the thermal activation, and H is the activation enthalpy (energy) which may be a function of the shear stress τ and the temperature T. For iron and steel in the temperature range of 80°-300°K, it has been found (Ref. 7) that H is primarily a function of the effective shear stress τ^*, given by the difference between the applied stress τ and the long range internal stress τ_μ (i.e., $\tau^* = \tau - \tau_\mu$).

Rearranging Eq. (2) and differentiating, one obtains

$$-\frac{dH}{d\tau^*} = kT\left(\frac{\partial \ln \dot{\gamma}/\nu}{\partial \tau}\right)_T = \frac{k \ln (\dot{\gamma}/\nu)}{\left(\frac{\partial \tau^*}{\partial T}\right)_{\dot{\gamma}}} \tag{3}$$

where $\nu = \rho bs\nu^*$ and $-dH/d\tau^*$ is defined as the activation volume v^*. Furthermore, from Eq. (2), one obtains

$$H = kT \ln (\nu/\dot{\gamma}) \tag{4}$$

It also follows that

$$T\left(\frac{\partial \tau^*}{\partial T}\right)_{\dot{\gamma}} \left(\frac{\partial \ln \dot{\gamma}/\nu}{\partial \tau}\right)_T = \ln (\dot{\gamma}/\nu) \tag{5}$$

Finally, one can show that (Ref. 19)

$$H = -kT^2\left(\frac{\partial \ln \dot{\gamma}/\nu}{\partial \tau}\right)_T \left(\frac{\partial \tau^*}{\partial T}\right)_{\dot{\gamma}} = -k\left(\frac{\partial \ln \dot{\gamma}/\nu}{\partial 1/T}\right)_{\tau^*} \tag{6}$$

From the above, it is evident that if ν is relatively independent of stress and temperature, the parameters H, v*, and ν can be obtained from the effect of temperature and strain rate on the yield or flow stress in a constant strain rate tension test or from the effect of stress and temperature on the strain rate in a constant stress creep test. For such determinations on polycrystalline iron, it is generally assumed that $\tau = (1/2)\sigma$ and $\dot{\gamma} = 0.7\dot{\epsilon}$, where σ is the tensile stress and $\dot{\epsilon}$ is the tensile strain rate. Also, $(\partial \tau^*/\partial T)_{\dot{\gamma}}$ is approximated by $(\partial \tau/\partial T)_{\dot{\gamma}}$, since $d\tau_\mu/dT$ is small compared to $(\partial \tau^*/\partial T)_{\dot{\gamma}}$.

Because σ_μ and k are relatively independent of temperature, the strong temperature dependence of the yield and flow stress in iron resides primarily in σ^*. It is therefore of importance to know the dislocation mechanism responsible for σ^*. Three mechanisms have been proposed:

a) Overcoming the Peierls-Nabarro stress (Refs. 9, 10, and 13).

b) Nonconservative motion of jogs in screw dislocations (Ref. 20).

c) Overcoming interstitial atom precipitates (Ref. 17).

One approach for determining the mechanism that is controlling is to determine the values of H, v*, and ν for yielding and flow, and compare these with predictions based on the specific dislocation models.

The results obtained for iron will now be discussed. Figure 1 gives the variation of the activation volume v^* for both yielding and flow in iron and steel with the effective stress τ^*.[1] The solid curve for the polycrystals is based on results by Conrad (Ref. 7) and Conrad and Frederick (Ref. 11). It is seen here that for the polycrystals v^* for yielding and flow decreases with stress from about 35 b^3 to 11 b^3 in the range $\tau^* = 2$ kg/mm^2 to $\tau^* = 45$ kg/mm^2. Below $\tau^* = 2$ kg/mm^2, v^* increases very rapidly with decrease in stress, becoming 200 b^3 or greater as τ^* approaches zero. It is further seen that the limited single crystal data (Refs. 17, 21, and 22) agree with the results for the polycrystals. Also, the activation volumes obtained from the dislocation mobility studies by Stein and Low (Ref. 23) are similar in magnitude to those obtained from the yield and flow stress data.

Figure 2 shows the effect of stress on the activation energy for yielding and flow. The solid curve represents results for polycrystalline material with total interstitial content (C + N + O) greater than 0.01 wt%. The dashed curve for stresses below 2 kg/mm^2 is for tests by Basinski and Christian (Ref. 10) on decarburized Ferrovac iron. Figure 2 shows that the activation energy for the not-decarburized material decreases from about 0.58 ev at $\tau^* = 0$ to 0.09 ev at $\tau^* = 45$ kg/mm^2.

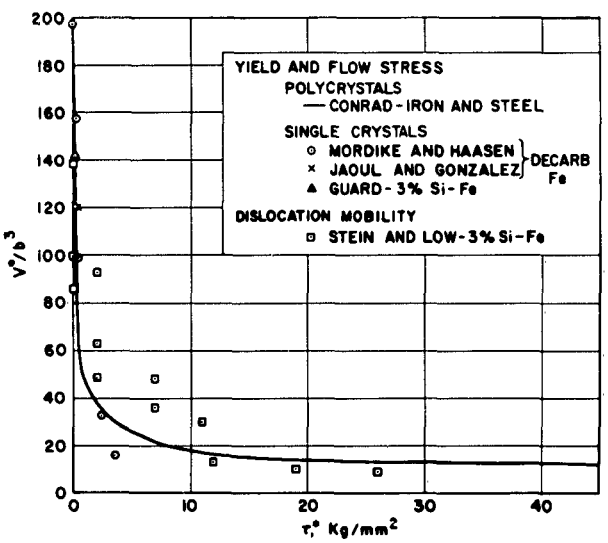

Figure 1. Effect of Stress on Activation Volume for Yielding and Flow in Iron and Steel

[1] To obtain τ^*, it was assumed that $\tau^* = 0$ when $(\partial\sigma/\partial T)_{\dot{\epsilon}}/\sigma \approx (d\mu/dT)/\mu$; i.e., when the temperature-dependence of the yield or flow stress is due principally to the change in shear modulus with temperature. For comparison with earlier work (Ref. 9), $\tau^* = \{(\tau - \tau^o) + 2$ kg/mm$^2\}$. For iron tested at a strain rate of 10^{-4} sec^{-1}, $\tau^* = 0$ at ~300°-350°K.

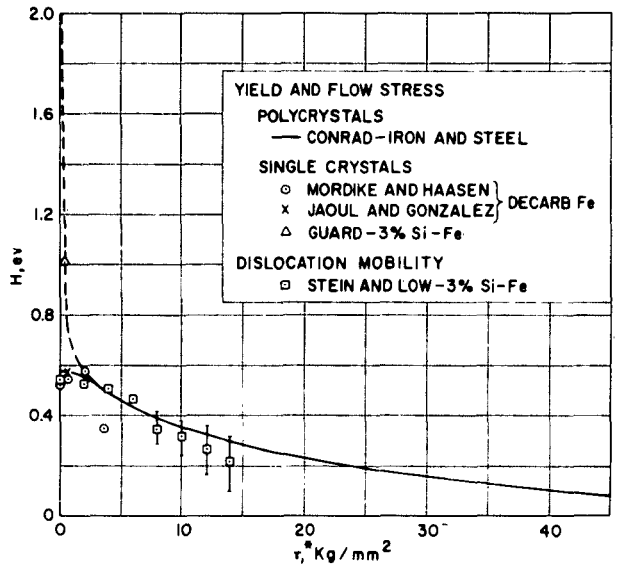

Figure 2. Effect of Stress on Activation Energy for Yielding and Flow in Iron and Steel

Again, the limited single crystal data and the dislocation mobility results yield values in reasonable agreement with the more numerous polycrystalline data.

According to Eq. (4), the value of ν can be obtained from the slope of a plot of H versus temperature. Furthermore, in the range where ν is a constant, H is proportional to the temperature T. This proportionality does not mean that H is a direct function of the temperature, but rather that H is a function of the stress, and to maintain a constant strain rate, the stress increases as the temperature decreases.

Figures 3 and 4 show plots of H versus temperature for various irons and steels (Refs. 10, 24, 25, 26, 27 and 28). It is here seen that H is proportional to the temperature to some value T^0, above which H either remains relatively constant at approximately 0.5-0.6 ev (not-decarburized material) or increases sharply to values of 2 ev or greater (decarburized material). The values of ν obtained from the initial straight line portions of these curves are between 6×10^6 and 6×10^9 sec^{-1}. Figure 5 gives plots of H versus T derived from the dislocation mobility studies of Stein and Low (Ref. 23) on 3.25 percent silicon iron. From the initial slope, one obtains a value of $\sim 10^6$ cm/sec for $\nu' = s\nu^*$. Taking $\nu = \rho b s \nu^*$, these values of ν and ν' give 10^8-10^{11} cm^{-2} for

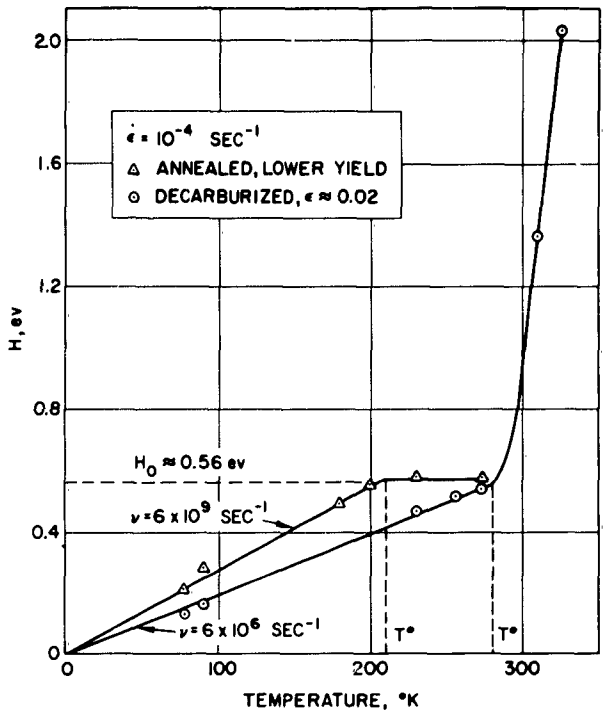

Figure 3. Variation of Activation Energy with Temperature for Decarburized Ferrovac Iron (Data from Ref. 10)

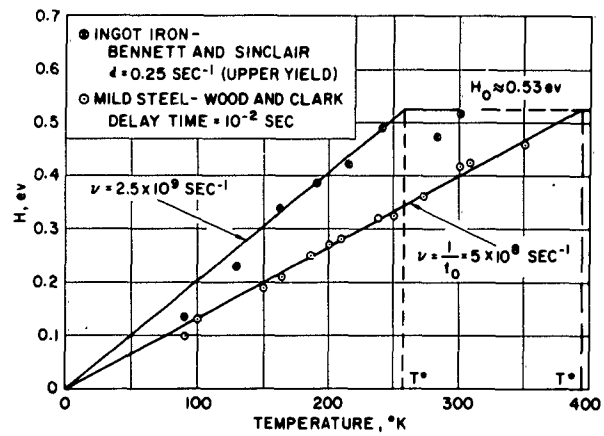

Figure 4. Variation of Activation Energy with Temperature for Ingot Iron and Mild Steel

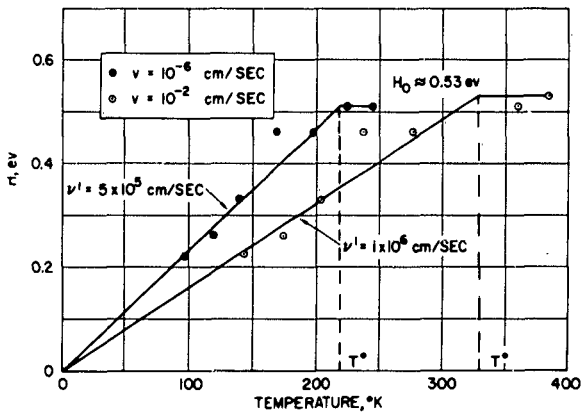

Figure 5. Variation of Activation Energy with Temperature for Dislocation Mobility in 3.25 percent Si-Fe (Data from Ref. 23)

the dislocation density ρ participating in the deformation. These densities are in reasonable agreement with values for iron obtained from internal friction studies (Ref. 29) and from direct observation of dislocations by thin film electron transmission (Ref. 30).

Lean, Plateau, and Crussard (Ref. 31) also found that the activation energy for the upper and lower yield stress of a mild steel is proportional to the temperature. For strain rates ranging from 10^{-5} to 10^{-1} sec^{-1}, they obtained H = 53 T cal/mole for the upper yield stress and H = 60 T cal/mole for the lower yield stress. Taking an effective strain rate given by the square root of the product of their maximum and minimum rates, one obtains $\nu = 5 \times 10^{8}$ sec^{-1} for the upper yield stress and $\nu = 10^{10}$ sec^{-1} for the lower yield stress. These values are in good agreement with those given in Figs. 3-5. Also, the fact that ν for the upper yield is less than that for the lower yield is consistent with the expectation that the dislocation density for the Luders strain is larger than that at the upper yield stress. Lean, Plateau and Crussard (Ref. 31) also found that the activation energy derived from the effect of strain rate on the ductile-to-brittle transition temperature was proportional to the temperature with a proportionality constant of 40-50, giving values of $\nu \approx 10^{8}$ sec^{-1}.

When comparing the values of H, v^* and ν with various thermally-activated dislocation mechanisms (overcoming the Peierls-Nabarro stress,[2] intersection of dislocations, nonconservative motion of jogs, cross-slip, overcoming precipitate particles, and breaking away from a Cottrell atmosphere), the best agreement is obtained with predictions based on overcoming some inherent lattice resistance such as the Peierls-Nabarro stress as the rate-controlling mechanism for both yielding (upper yield, delay time for yielding, lower yield, Luders band propagation) and flow (flow stress and dislocation mobility) in iron (Refs. 9 and 11). Support for the Peierls-Nabarro stress mechanism is also provided by the observation of Low and Guard (Ref. 32) that dislocations in silicon-iron lie along close-packed directions. The experimental data thus suggest that the strong temperature and strain-rate dependence of the yield and flow stress in iron arises from a high Peierls-Nabarro stress in the b.c.c. lattice.

If σ^* represents the thermally-activated overcoming of the Peierls-Nabarro stress, one must explain why σ^* may vary with strain, composition, grain size, precipitates, etc., since one does not expect the Peierls-Nabarro stress to be affected by the structure. In regard to this, recent work by Conrad and Frederick (Ref. 11) has shown that the effect of strain on the temperature dependence of decarburized iron or quenched iron can be explained simply by an increase in the number of dislocations ρ contributing to the deformation. It was found that neither H nor v^* were affected by straining, the only affect being on ν, or more specifically on the dislocation density ρ. An example of the change in ν with strain is shown in Fig. 6 for the data by Basinski and Christian (Ref. 10) on their decarburized Ferrovac iron. Similarly, the stronger temperature dependence of σ^* observed by Basinski and Christian

[2] A thermally-activated mechanism for overcoming the Peierls-Nabarro stress has been proposed by Seeger (Ref. 59). It involves the formation of a pair of kinks in a dislocation line lying along a close-packed direction and the subsequent lateral propagation of the kinks along the dislocation line.

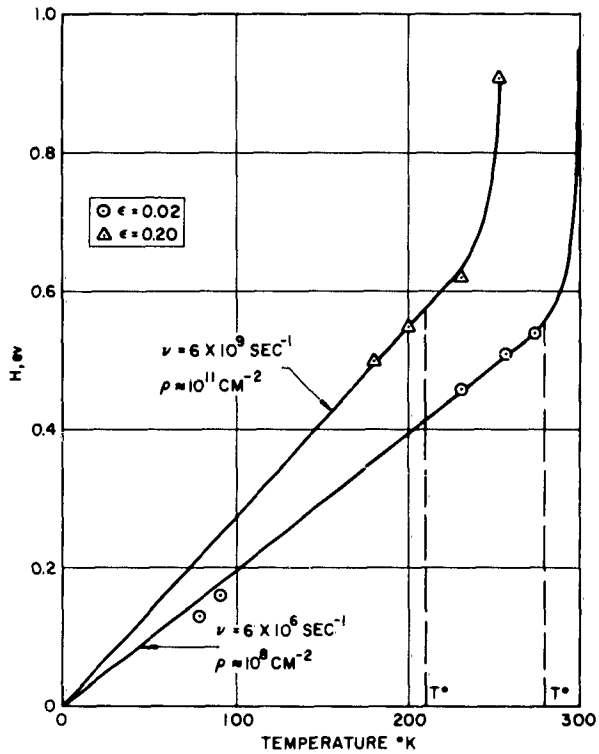

Figure 6. Variation of Activation Energy with Temperature for Ferrovac Iron (From data of Ref. 10)

for their decarburized iron as compared to their annealed (not-decarburized) iron was due to a larger value of ν, i.e., a higher dislocation density for the annealed material (Fig. 3). Likewise, the stronger temperature dependence of σ^* (given by taking $\sigma_T - \sigma_{300}$) for the decarburized material in Fig. 32 of Ref. 2 by Low, as compared to the not-decarburized material, is probably due to a smaller value of ν for the decarburized material. These results suggest that interstitial precipitates play a significant role in the generation of dislocations, agreeing with observations by Leslie (Ref. 33) in thin-film electron transmission studies on iron containing carbon and nitrogen precipitates (for example, Fig. 7).

Since heating and quenching from a high temperature will also remove interstitial precipitates, it is expected that the temperature dependence of σ^* for iron with low interstitial contents will be smaller for slow cooling than for quenching rapidly from a high temperature. This has been found to be the case for specimens of vacuum-melted electrolytic iron (C + N $\approx$ 0.015 percent) heated to 920°C and then either water-quenched or slowly cooled and aged (Ref. 11).

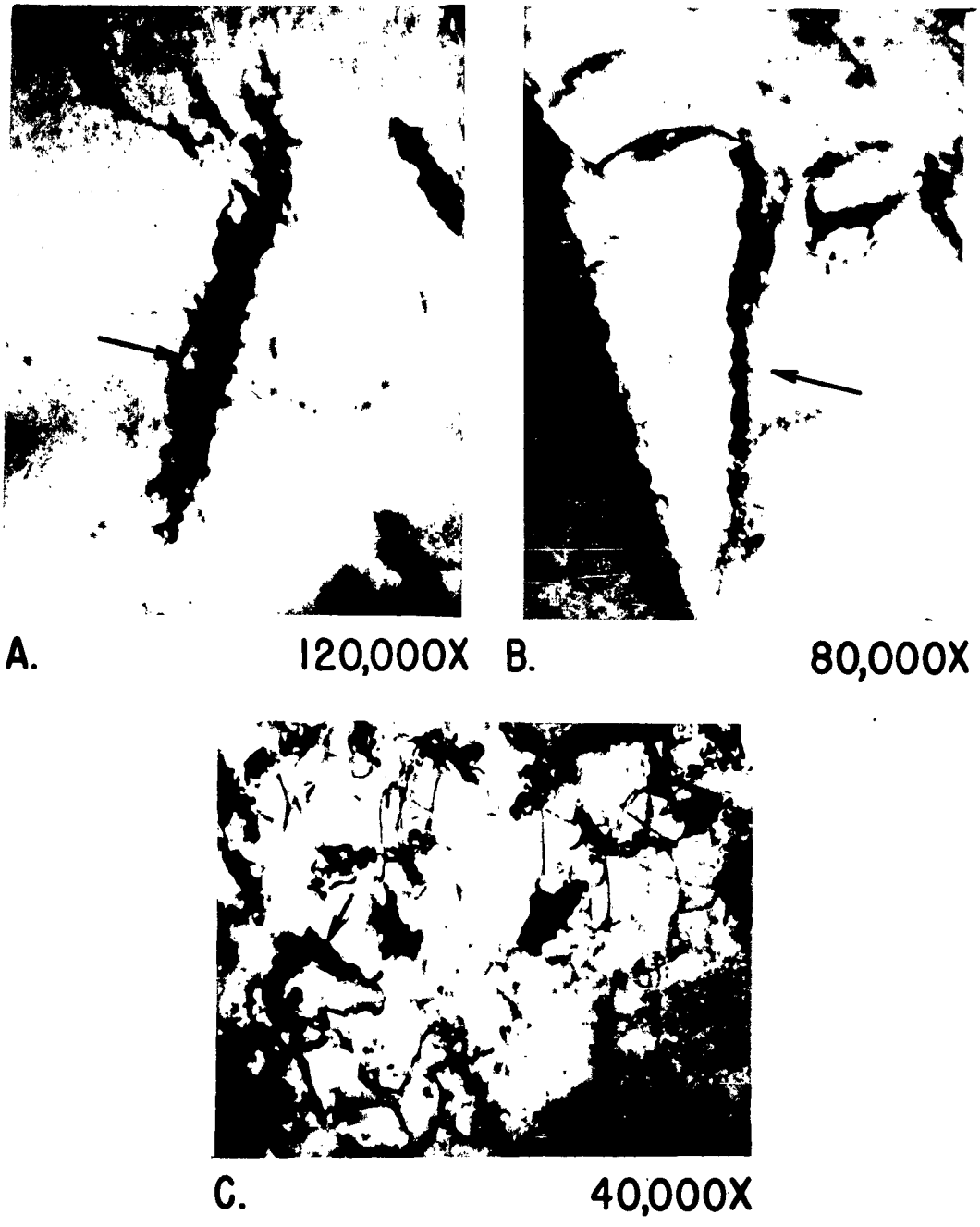

Figure 7. Fe_3C Particles Acting as Dislocation Sources in an Fe-Mn-C Alloy. (After Leslie, Ref. 33).

Along these lines one can also understand why σ^* for annealed iron and steel is relatively independent of strain, while σ^* for the decarburized or quenched material changes with strain (Refs. 7, 10, and 11). Due to the presence of precipitates in the annealed material, a large number of dislocations ($\sim 10^{10}$ to 10^{11} cm^{-2}) are already produced during the lower yield point elongation and no significant increase occurs upon further straining. On the other hand, in the quenched or decarburized material where no precipitates are present, the number of places where dislocations can be generated are fewer and hence the density of dislocations existing at the yielding stress is lower (of the order of 10^8 cm^{-2}). Upon straining, this density then increases to approximately 10^{11} cm^{-2} (Fig. 6), giving a decrease in σ^*.

On the basis of the above, it is expected that the weaker temperature dependence of the yield stress of single crystals as compared to polycrystals (Ref. 8; also Fig. 17 in Ref. 2) in the 100°-300°K range is due to a larger value of ν for single crystals (Ref. 9). For example, for the difference in τ^* at 100°K between single and polycrystals (~ 7 kg/mm^2), one obtains $\nu_s/\nu_p \approx 10^3$ from the variation of H with τ^* in Fig. 2. This difference in ν can be due to a difference in dislocation density ρ or to a difference in the average distance s the dislocations move forward per successful thermal fluctuation. If the average free length of a dislocation loop in a single crystal is larger than that in a polycrystal, a difference in s will result; this has been observed to be the case (Ref. 30). Similarly, one can explain the weaker temperature dependence of the yield stress of high purity polycrystals as compared to impure polycrystals over the range of 100°-300°K (Refs. 8 and 9). However, if the Peierls-Nabarro model presented above is valid and twinning does not occur, the yield stress of single crystals and high purity polycrystals must then rise more rapidly than that of the impure polycrystals below about 100°K, since the value of the stress at 0°K must be the same for all forms of iron. This is shown schematically in Fig. 8. Some indication that this does actually occur is provided by the yield stress data of Allen, Hopkins and McLennan

(Ref. 34) on iron single crystals and Lawley, Van den Sype and Maddin (Ref. 35) on molybdenum single and polycrystals. Additional experiments on the effect of temperature and strain rate on the yield and flow stress of single crystals and high purity polycrystals are needed to resolve the question of the weaker temperature dependence of the yield and flow stress of these materials as compared to impure polycrystals.

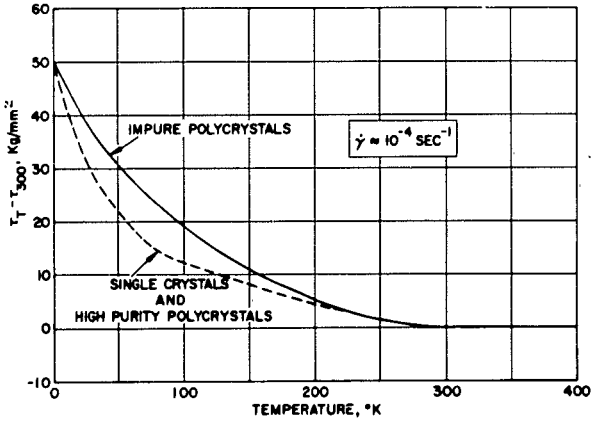

Figure 8. Schematic of Temperature Dependence of the Yield Stress of Iron Single and Polycrystals

IV. INTERPRETATION OF σ_μ

As indicated above, σ_μ is affected by C+N in solution, interstitial precipitates, and strain. A review of these effects and their interpretation in terms of dislocation behavior will now be discussed.

A. EFFECT OF C + N IN SOLUTION

Figure 9, taken from the work of Heslop and Petch (Ref. 13), shows how $\sigma_o = \sigma^* + \sigma_\mu$ varies with the amount of C + N in solution. It is seen here that σ_o increases in proportion to the amount of C + N in solution and independently of the temperature; i. e., only the athermal component of the yield stress σ_μ is influenced by the C + N in solution. Cracknell and Petch (Ref. 12) and Heslop and Petch (Ref. 13) attribute this increase to the resistance of C and N atoms to the motion of dislocations. Using the method of Mott and Nabarro (Refs. 35 and 36) for the motion of dislocations through finely dispersed centers of internal stress, they calculated that the effect should be proportional to the concentration, just athermal, and give a stress increase of about 4-10 kg/mm^2 for 0.25 percent C (all in agreement with the experimental observations).

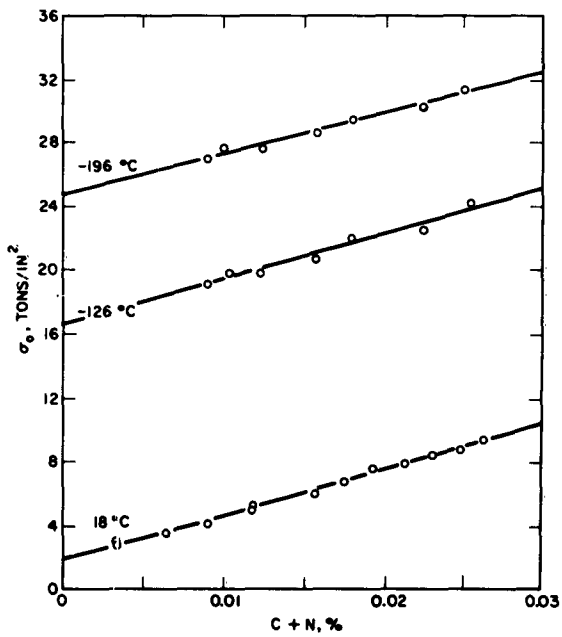

Fig. 9. Effect on $\sigma_o = \sigma^* + \sigma_\mu$(st) of C + N in Solution (Ref. 13)

On the other hand, Schoeck and Seeger (Ref. 37) suggest that the effect on σ_μ of C + N in solution is due to the resistance to dislocation motion associated with stress-induced ordering of the interstitials in the stress field of a dislocation. Since both the strength and radius of an atmosphere of ordered interstitials are inversely proportional to the temperature, the increase in yield strength due to this effect is temperature independent. Assuming that the increase in σ_μ because of C + N in solution is due to the stress-induced ordering of interstitials, they calculated

$$\tau_\mu = 38 \times 10^{-20} \, f/ba_o^3 \text{ dynes/cm}^2 \qquad (7)$$

where f is the atomic fraction of interstitials, a_o is the lattice constant, and b is the Burgers vector. Substituting into this equation, they obtained values of σ_μ in agreement with the yield stress of single crystals in the temperature range where the stress is relatively independent of temperature, i.e., at $T \approx 300^\circ K$ for $\dot{\epsilon} = 10^{-4} \text{ sec}^{-1}$. Also, their calculations predicted that $d\sigma_\mu/dc = 65 \text{ kg/mm}^2/\text{at. \%}$, in good agreement with the experimentally observed value of $d\sigma_\mu/dc = 45 \text{ kg/mm}^2/\text{at.\%}$ in Fig. 9. Additional support for the Schoeck and Seeger mechanism is provided by the work of Wilson and Russell (Ref. 38). They found that a part of the increase in yield stress during strain-aging of a low carbon steel developed too rapidly to be explained by long-range diffusion of C and N to the dislocations. The rate at which the initial rise in yield strength developed[4] and the dependence of its magnitude on the dissolved C + N content were in good agreement with the increase expected due to the stress-induced ordering of interstitials in the stress field of a dislocation.

---

*To reform an atmosphere of ordered interstitial atoms, the interstitials in the immediate vicinity of a dislocation need make only one atomic jump.

In view of the above, it is evident that additional work is needed to identify positively the mechanism responsible for the increase in yield stress due to C + N in solution.

B. EFFECT OF PRECIPITATES

That precipitates of C and N contribute to the athermal component of the yield stress is shown in Fig. 10. The effect of interparticle spacing on σ_μ was investigated by Leslie (Ref. 33) for carbide particles and Keh and Wriedt (Ref. 39) for nitride particles, using electron transmission. Their results are given in Figs. 11 and 12. It is seen from the graphs on the left side of these figures that the relationship between interparticle spacing λ and the yield strength can be considered to obey Orowan's equation (Ref. 40) for the shear stress τ required to bow a dislocation between the particles, namely,

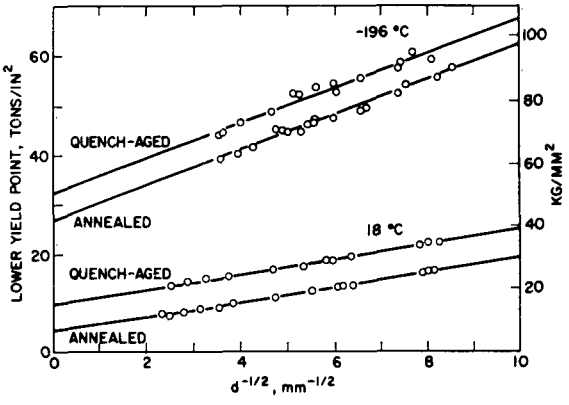

Fig. 10. Effect of Quench-Aging on Lower Yield Stress of Mild Steel (Ref. 13)

$$\tau = \tau_o + \alpha\mu b/\lambda \quad . \tag{8}$$

τ_o is the shear stress required to move a dislocation in the absence of particles, α is a constant of the order of 1/2, μ is the shear modulus, and b is the Burgers vector. Substituting $\mu = 7.8 \times 10^3$ kg/mm^2, $b = 2.48 \times 10^{-8}$ cm, $\alpha = 1/2$, and $\sigma = 2\tau$ into Orowan's equation, one obtains a value in reasonable agreement with the experimental results of 1.93×10^{-4} kg/mm^2/cm for the slope of σ_{ly} versus $1/\lambda$. Also, there is good agreement between the extrapolated values of the lower yield stress for $\lambda^{-1} = 0$ and the experimental values of the as-quenched or over-aged conditions.

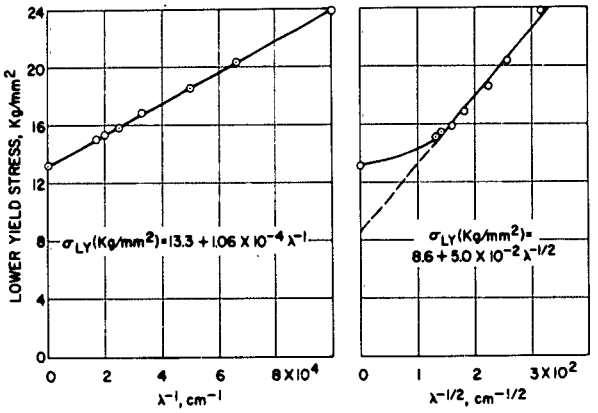

Fig. 11. Relationship Between Yield Stress and Carbide Spacing in a Quench-Aged Fe–0.45 Mn–0.017C Alloy (Ref. 33)

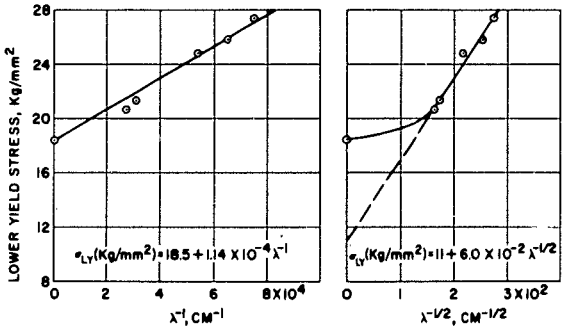

Fig. 12. Relationship Between Yield Stress and Nitride Spacing in a Quench-Aged Fe–0.022 Percent N Alloy (Ref. 39)

More recently Ansel and Lenell (Ref. 41) have proposed that yielding in dispersion-hardened materials occurs when the shear stress due to piled-up groups of dislocations held up at the dispersed particles is sufficient to either plastically deform or fracture the particles. This leads to the following relationship between the yield stress and the particle spacing:

$$\tau = \tau_o + \sqrt{\mu\ \mu^*/2a}\,\lambda^{-1/2} \qquad (9)$$

where μ is the shear modulus of the matrix, μ^* is the shear modulus of the particle and a is a proportionality constant dependent on the crystal perfection of the dispersed particles. To check this relationship, a plot of yield stress versus $\lambda^{-1/2}$ is given in the right of Figs. 11 and 12. It is seen here that the extrapolations to $\lambda^{-1/2} = 0$ do not agree with values of the stress for the quenched or over-aged condition, although Eq. (8) can be considered to be obeyed over the range of interparticle spacings investigated. Because the values of μ^* and a are not known for iron carbide and nitride particles, the theory cannot be checked from the value of the slope of the plots of σ versus $\lambda^{-1/2}$.

C. EFFECT OF STRAIN

Keh and Weissman (Ref. 30) report that the dislocations for the most part are relatively straight and lie on crystallographic plans for the deformation of polycrystalline iron at low temperatures (140°K). On the other hand, at 300°K they cluster inside the individual grains to form cells where the cell walls consist of a tangled network of dislocations. The tendency to form cells is a function of strain as well as deformation temperature, occurring at larger strains for lower temperatures.

If the effect of strain on σ_μ is due to the long-range stress fields associated with dislocations on parallel planes, then this contribution to σ_μ is given by (Ref. 35):

$$\tau_\mu = \alpha \mu b \rho^{1/2} \tag{10}$$

where α is a constant of the order of 0.1 and ρ is the density of dislocations, which increases with strain. An analysis by Li (Ref. 42) of the stress field in the interior of the cells due to the cell walls (consisting of crossed grids of screw dislocations) yields a similar increase in flow stress with dislocation density. Thus, it appears that the effect of strain on σ_μ is given by Eq. (10) (ρ increasing with strain), irrespectively of whether the dislocations are relatively straight on parallel slip planes or are in the form of tangles in cell walls; the only difference for the two distributions is perhaps in the constant α.

Figure 15 of Ref. 2, taken from the work of Keh and Weissman (Ref. 30), shows that the flow stress of deformed iron increases with dislocation density according to Eq. (10), giving a value of $\alpha = 0.38$. This and the fact that the strain hardening in iron is relatively independent of temperature suggest that the increase in σ_μ with strain is principally due to long-range stress fields. In agreement with this is the fact that slip in single crystals and

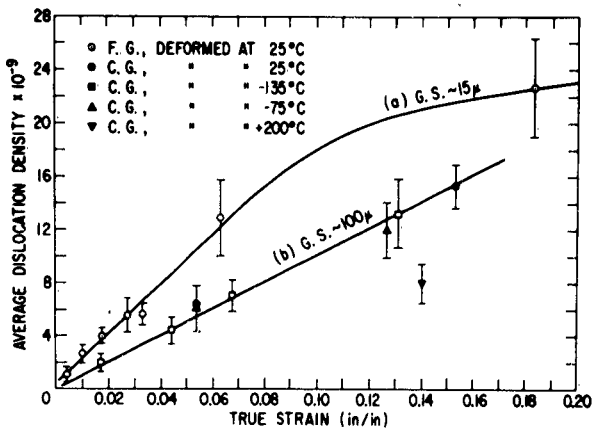

Fig. 13. Relationship Between Average Dislocation Density and Plastic Strain in Iron (Ref. 30)

polycrystalline grains of iron occurs principally on a single surface consisting of the most favorable oriented slip vector and the plane of maximum shear stress; very little slip occurs on any other plane (Ref. 18). Finally, the parabolic form of the stress-strain curves for iron (Ref. 18) are in agreement with Eq. (10) and the observed increase in dislocation density with strain given in Fig. 13.

D. COMBINED EFFECT OF C + N IN SOLUTION, PRECIPITATES, AND STRAIN

It is expected that the combined effect of the C + N in solution, precipitates, and strain on σ_μ is given by the sum of the individual contributions and, hence, choosing the mechanisms which seem most plausible at the present time, we have

$$\tau_\mu = a_1 \mu b \rho^{1/2} + a_2 b \lambda^{-1} + \frac{a_3 f}{b a_o^3} \qquad (11)$$

where a_1 and a_2 are constants of the order 0.3-0.4, $a_3 \approx 38 \times 10^{-20}$ dynes cm^2, f is the atomic fraction of interstitial atoms, and a_0 is the lattice constant.

V. INTERPRETATION OF k

The model of yielding proposed by Cottrell (Ref. 6) is shown schematically in Fig. 14. Due to the elastic interaction between C and N and the dislocations in iron, these interstitials segregate to the dislocations and lock them. During the initial loading of a specimen below the upper yield stress, some dislocations are torn from their interstitial atmospheres at regions of stress concentration (for example, at S_1) and act as sources for the generation of additional dislocations.

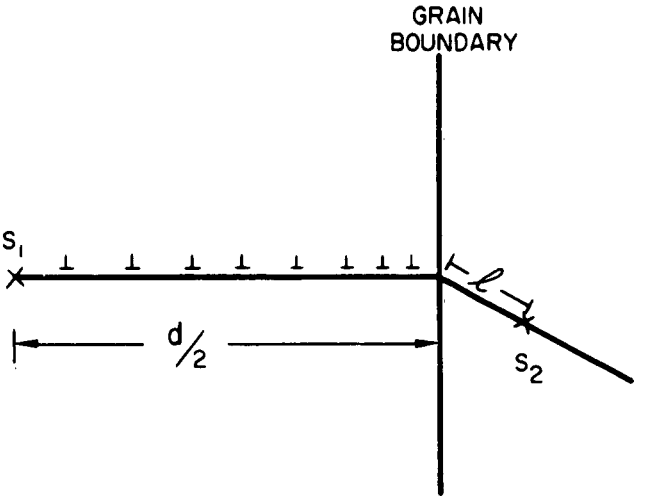

Fig. 14. Schematic of Model Proposed by Cottrell (Ref. 6) for Yielding in Iron and Steel

The newly generated dislocations then move along the slip plane and pile up at some strong obstacle (such as a grain boundary) where they exert a stress concentration whose value at a distance ℓ ahead of the pile-up is given by $(\tau = \tau_i)(d/2\ell)^{1/2}$. Here τ is the applied shear stress, d is the grain diameter, and τ_i represents the resistance of the lattice to the motion of dislocations from S_1 to the grain boundary. Yielding occurs at S_2 (the location of another locked dislocation in the next grain at a distance ℓ from the boundary) when the total stress there is sufficient to tear the dislocation from its atmosphere with the aid of thermal fluctuations. If τ_ℓ is the unlocking stress at S_2, one obtains

$$(\tau - \tau_i)(d/2\ell)^{1/2} + \tau = \tau_\ell \qquad (12)$$

If $d >> \ell$, this becomes

$$\tau = \tau_i + (2\ell)^{1/2} \tau_\ell \, d^{-1/2} \tag{13}$$

which is identical to Eq. (1) with $\tau_i = 1/2\{\sigma^* + \sigma_\mu(st)\}$ and $k = 2(2\ell)^{1/2}\tau_\ell$.

Some support for the above interpretation of k is provided by the fact that the value of τ_ℓ derived from experimental values of k is in agreement with that expected from theoretical considerations (Ref. 6). In agreement with the model, k also decreases significantly as the C and N contents are decreased by decarburization (Ref. 43). However, two experimental facts are not in accord with Cottrell's model of yielding:

a) k is relatively independent of temperature and strain rate in the range of 100°-300°K (Refs. 7, 14, and 44), which is not expected from the analyses of unlocking by Cottrell and Bilby (Ref. 45), Fisher (Ref. 46) and Cottrell (Ref. 47).

b) k is approximately the same for the flow stress beyond the lower yield stress as it is for the lower yield stress (Refs. 7 and 16). This is not expected if yielding represents the unlocking of dislocations and flow represents the motion of free dislocations.

The first discrepancy can be explained if the unlocking at S_2 is athermal rather than thermal, e.g., the interstitial atmosphere may be so wide that thermal fluctuations do not play a significant role during unlocking. Some indication that this may be the case for a Cottrell type atmosphere is provided by the work of Cochardt, Schoeck and Wiedersich (Ref. 48), which shows that the slip plane, as well as immediately below the extra half-plane of the dislocation, are equally favored sites for interstitials. Also, if the atmosphere is a Snoek-type (ordered interstitials in the stress field of a dislocation), the unlocking would be athermal (Ref. 32).

An explanation for the second discrepancy is that unlocking occurs during flow as well as during yielding (Refs. 16 and 43). Also, there is some question as to whether k is the same for the flow stress as the yield stress (Ref. 43). If these explanations are valid, the Cottrell model could therefore still apply. However, several other observations suggest that unlocking of dislocations is not responsible for the yield point in iron:

a) In LiF crystals exhibiting a yield-point behavior, the original pinned dislocations remain locked and do not participate in the yielding (Ref. 49). There is some indication that this is also the case for fully pinned dislocations in iron and steel (Ref. 50).

b) In iron and steel exhibiting a yield point, the dislocations are often pinned by precipitates rather than an interstitial atmosphere (Refs. 30, 33, and 39). It is difficult to imagine that a Cottrell-Bilby (Ref. 45) type of unlocking is operative in such cases.

c) Dislocation pile-ups have not been observed in polycrystalline iron either by etch-pits (Ref. 51) (3 percent silicon-iron) or by electron transmission microscopy (Ref. 30).

The evidence is thus rather strong that in iron and steel k is not a measure of the stress to unlock dislocations from an interstitial atmosphere.

Four alternative explanations that do not involve the unlocking of dislocations have been proposed for the effect of grain size on the yield and flow stress:

a) The increase in stress with decrease in grain size results from the fact that different thermal treatments used to obtain different grain sizes yield different dislocation or precipitate structures (Ref. 7).

b) k represents the stress to athermally generate dislocations from the grain boundary or its immediate vicinity (Ref. 7).

c) k is a measure of the energy associated with the additional grain boundary surface area formed when slip bands penetrate the boundary (Ref. 52).

d) k is related to the strong work-hardening in the vicinity of a grain boundary due to the complexity of slip which occurs there (Ref. 53).

At present there is insufficient evidence to fully substantiate any of these ideas.

VI. INTERPRETATION OF THE YIELD POINT

As indicated above, numerous experimental data suggest that the yield point in iron and steel is not due to the thermally-activated tearing of dislocations from their interstitial atmosphere. This is pointed out in Ref. 9. It is postulated that the yield point in iron and steel may be of the type proposed by Johnson and Gilman (Ref. 49) for the yield point in LiF, i. e., it results from the lower average velocity of dislocations required to maintain a constant strain rate when there occurs a sudden multiplication of dislocations by some mechanism such as the double cross-slip mechanism of Koehler (Ref. 54) and Orowan (Ref. 40). Three factors favor the occurrence of such a yield point:

a) Initially there should exist only a small number of dislocations which can contribute to the plastic flow.

b) The dislocation density contributing to the plastic flow should increase very rapidly with strain.

c) The change in stress for a given change in dislocation velocity ($\partial\sigma/\partial \ln v$ or $\partial\sigma/\partial \ln \dot{\epsilon}$) should be relatively large.

All three of these are found in iron or steel exhibiting a yield point. A low initial dislocation density results from the fact that the original dislocations are pinned by an interstitial atmosphere or precipitates. A rapid increase of dislocation density with strain is indicated by the data in Fig. 13 and, furthermore, is suggested by the observations of Low and Guard (Ref. 32) on the multiplication of dislocations in silicon-iron. Finally, the change in stress for a given change in strain rate, $(\partial\sigma/\partial \ln \dot{\epsilon})$ is larger for iron than for the close-packed metals which do not normally exhibit a yield point. For example, for a strain rate of $10^{-4}\,\mathrm{sec}^{-1}$ at $200^{\circ}\mathrm{K}$, $\partial\sigma/\partial \ln \dot{\epsilon}$ for iron is $1.74\ \mathrm{kg/mm}^2$ (Ref. 9) at the yield stress, while it is $\sim 0.02\ \mathrm{kg/mm}^2$ for copper (Ref. 55). The conditions are thus favorable for the occurrence of a Johnson-Gilman type yield point in iron and steel.

To check this interpretation of the yield point, stress-strain curves are calculated for mild steel at several temperatures from the available information on dislocation density, dislocation mobility, and strain-hardening in iron and steel. The exact procedure and equations employed are given in the appendix. The curves are calculated for a strain rate of 10^{-3} sec^{-1} and for temperatures below 250°K. i.e., for the temperature range where the activation energy is proportional to the temperature (or the stress range where $\tau > \tau^{o}$, and τ^{o} is defined as the stress at 300°K for a strain rate of ~1 sec^{-1} (Ref. 9)). Figure 15 shows the calculated stress-strain curves. The experimental curves are also given for comparison. Agreement between the calculated and experimental stress-strain curves is exceptionally good, especially in view of some of the assumptions which were made in the calculations.

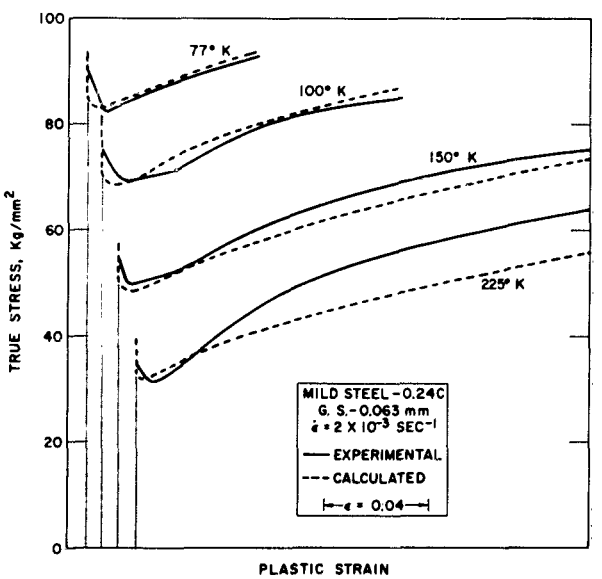

Figure 15. Comparison of Calculated and Experimental Stress-Strain Curves for Mild Steel

APPENDIX

PROCEDURE EMPLOYED TO CALCULATE THE STRESS-STRAIN CURVES

The stress-strain curves were calculated on the basis of the relationship

$$\sigma = \sigma^*(\epsilon) + \sigma_\mu^o + \sigma_\mu(\epsilon) \tag{A-1}$$

where σ^* is the thermal component of the stress that is dependent on the strain ϵ through the dislocation density ρ contributing to the plastic flow, σ_μ^o is the initial athermal component of the stress, and σ_μ is the increase in the athermal component due to strain hardening. To obtain σ^* as a function of strain, it was assumed that the dislocation density ρ contributing to the plastic flow was the same as the total dislocation density measured by Keh and Weissmann (Ref. 30) (Fig. 13, this paper) and was given by

$$\rho = \frac{\beta\epsilon}{bd^{1/2}} \tag{A-2}$$

where $\beta = 70\ \text{mm}^{-1/2}$, b is the Burgers vector, and d is the grain size. Inserting this value for ρ in Eq. (4) of the text gives

$$H(\tau^*) = kT\ell n\frac{\beta s\nu^*\epsilon}{d^{1/2}\dot{\epsilon}} \tag{A-3}$$

Taking $s\nu^* = 10^6$ cm/sec from the dislocation mobility data by Stein and Low (Ref. 23) (Fig. 5, this paper), the change in $H(\tau^*)$ with strain was calculated for a given temperature, grain size, and strain rate. Having established the variation of $H(\tau^*)$ with strain, the change in σ^* (equal to $2\tau^*$) with strain was determined from the solid curve relating H and τ^* given in Fig. 2 of the

text. σ_μ^o was taken as the lower yield stress at 300°K corrected for the strain hardening associated with the lower yield point elongation by substituting ρ from Eq. (A-2) into Eq. (10) of the text, with $\alpha = 0.38$. The increase in σ_μ with strain was also obtained by substituting ρ from Eq. (A-2) into Eq. (10). The stress-strain curves were then determined by adding the values of σ^*, σ_μ^o, and σ_μ for each value of strain. Since only plastic strain was considered, the upper yield point was taken as the stress at a plastic strain of 10^{-4}. This is approximately the observed pre-yield microstrain (Ref. 56-58).

REFERENCES

1. Allen, N. P., contribution to High Purity Iron and Its Dilute Solid Solutions (Interscience Publishers, Inc., New York, 1963).
2. Low, J. R., contribution to High Purity Iron and Its Dilute Solid Solutions (Interscience Publishers, Inc., New York, 1963).
3. Hall, E. O., Proc. Phys. Soc. B64, 747 (1951).
4. Petch, N. J., J. Iron and Steel Inst. 174, 25 (1953).
5. Petch, N. J., Progr. in Metal Phys. 5, 1 (1954).
6. Cottrell, A. H., Trans. AIME 212, 192 (1958).
7. Conrad, H., and G. Schoeck, Acta Met. 8, 791 (1960).
8. Conrad, H., Phil. Mag. 5, 745 (1960).
9. Conrad, H., J. Iron and Steel Inst. 198, 364 (1961).
10. Basinski, Z. S., and J. W. Christian, Australian J. Phys. 13, 299 (1960).
11. Conrad, H., and S. Frederick, Acta Met. 10, 1013 (1962).
12. Cracknell, A., and N. J. Petch, Acta Met. 3, 186 (1955).
13. Heslop, J., and N. J. Petch, Phil. Mag. 1, 866 (1956).
14. de Kazinski, F., W. A. Backofen and B. Kapadia, contribution to Fracture (John Wiley and Sons, Inc., New York, 1959), p. 65.
15. Petch, N. J., contribution to Fracture (John Wiley and Sons, Inc., New York, 1959), p. 54.
16. Armstrong, R. W., and N. J. Petch, Westinghouse Scientific Paper 10-01000-0-PI (29 December 1959).
17. Mordike, B. L., and P. Haasen, Phil. Mag. 7, 459 (1962).
18. Jaoul, B., J. Mech. and Phys. Solids 9, 69 (1961).
19. Conrad, H., and H. Wiedersich, Acta Met. 8, 128 (1960).

20. Schoeck, G., Acta Met. 9, 382 (1961).

21. Jaoul, B., and D. Gonzalez, J. Mech. and Phys. Solids 9, 16 (1961).

22. Guard, R., Acta Met. 9, 163 (1961).

23. Stein, D.F., and J.R. Low, J. Appl. Phy. 31, 362 (1960).

24. Bennett, P.E., and G.M. Sinclair, Theoretical and Applied Mechanics Report 157, University of Illinois, Urbana (1959).

25. Clark, D.S., and D.S. Wood, Am. Soc. Testing Materials, Proc. 49, 717 (1949).

26. Wood, D.S., and D.S. Clark, Trans. Am. Soc. Metals 43, 571 (1951).

27. Wood, D.S., and D.S. Clark, Trans. Am. Soc. Metals 44, 726 (1952).

28. Clark, D.S., Trans. Am. Soc. Metals 46, 34 (1954).

29. Harper, S., Phys. Rev. 83, 709 (1951).

30. Keh, A., and S. Weissmann, contribution to Proceedings of the Conference on the Impact of Transmission Electron Microscopy on Theories of the Strength of Crystals, eds. G. Thomas and J. Washburn (Interscience Publishers, Inc., New York, 1963).

31. Lean, J.B., J. Plateau and C. Crussard, Mem. sci. revue. metall. 56, 427 (1959).

32. Low, J.R., and R.W. Guard, Acta Met. 7, 171 (1959).

33. Leslie, W.C., Acta Met. 9, 1004 (1961).

34. Allen, N.P., B.E. Hopkins and J.E. McLennan, Proc. Roy. Soc. (London) 234, 221 (1956).

35. Lawley, A., J. Van den Sype, and R. Maddin, J. Inst. Metals 91, 23 (1962).

36. Mott, N.F., and F.R.N. Nabarro, Report of the Conference on Strength of Solids (Physical Society, London, 1948), p. 1.

37. Mott, N.F., contribution to Imperfections in Nearly Perfect Crystals (John Wiley and Sons, Inc., New York, 1952), p. 173.

38. Schoeck, G., and A. Seeger, Acta Met. 7, 469 (1959).

39. Wilson, D.V., and B. Russell, Acta Met. 7, 628 (1959).

40. Keh, A.S., and H.A. Wriedt, Trans. AIME 224 (3), 560-572 (1962).

41. Orowan, E., Dislocations in Metals (AIME, New York, 1954), p. 69.

42. Ansell, G.S., and F.V. Lenel, Acta Met. 8, 612 (1960).

43. Li, J.C.M., contribution to Direct Observation of Imperfections in Crystals (Interscience Publishers, Inc., New York, 1962), p. 234.

44. Armstrong, R., et al., Phil. Mag. 7, 45 (1962).

45. Heslop, J., and N.J. Petch, Phil. Mag. 3, 1128 (1958).

46. Cottrell, A.H., and B.A. Bilby, Proc. Phys. Soc. (London) 62A, 49 (1949).

47. Fisher, J.C., Trans. Am. Soc. Metals 47, 451 (1955).

48. Cottrell, A.H., Report on the Conference on High Rates of Strain (Institute of Mechanical Engineers, London, 1957), p. 448.

49. Cochardt, A.W., G. Schoeck and H. Wiedersich, Acta Met. 3, 533 (1955).

50. Johnson, W.G., and J.J. Gilman, J. Appl. Phys. 30, 129 (1959).

51. Leslie, W.C., and A.S. Keh, "An Electron Transmission Study of the Strain-Aging of Iron," U.S. Steel Report (June 1961).

52. Suits, J.C., and B. Chalmers, Acta Met. 9, 854 (1961).

53. Russell, T.L., D.S. Wood and D.S. Clark, Acta Met. 9, 1054 (1961).

54. Johnson, A.A., Phil. Mag. 7, 177 (1962).

55. Koehler, J.S., Phys. Rev. 86, 52 (1952).

56. Carreker, R.P., Jr., and W.R. Hibbard, Jr., Acta Met. 1, 654 (1953).

57. Hendrickson, J.A., D.S. Wood and D.S. Clark, Acta Met. 4, 593 (1956).

58. Wessel, E.T., Trans. AIME 209, 930 (1957).

59. Owen, W., M. Cohen and B. Averbach, Trans. Am. Soc. Metals 50, 517 (1958).

60. Seeger, A., Phil. Mag. 1, 651 (1956).

Aerospace Corporation, El Segundo, California. YIELDING AND FLOW OF IRON, prepared by H. Conrad. 27 February 1963. [39] p. incl. illus. (Report TDR-169(3240-11)TN-2;SSD-TDR-63-27) (Contract AF 04(695)-169) Unclassified report

The significance of the parameters of the Hall-Petch equation for yielding and flow of iron and steel are discussed. The available experimental data suggest that σ^* represents the thermally-activated overcoming of the Peierls-Nabarro stress. The variations in σ^* with structure can be interpreted as changes in either dislocation density contributing to the deformation or the average distance the dislocations move per successful thermal fluctuation. Good agreement between experiment and theory is found for the contributions to σ_μ of interstitials in solution, precipitate particles, and strain. The significance of k is still unresolved. The experimental data suggest that

(over)

UNCLASSIFIED

Aerospace Corporation, El Segundo, California. YIELDING AND FLOW OF IRON, prepared by H. Conrad. 27 February 1963. [39] p. incl. illus. (Report TDR-169(3240-11)TN-2; SSD-TDR-63-27) (Contract AF 04(695)-169) Unclassified report

The significance of the parameters of the Hall-Petch equation for yielding and flow of iron and steel are discussed. The available experimental data suggest that σ^* represents the thermally-activated overcoming of the Peierls-Nabarro stress. The variations in σ^* with structure can be interpreted as changes in either dislocation density contributing to the deformation or the average distance the dislocations move per successful thermal fluctuation. Good agreement between experiment and theory is found for the contributions to σ_μ of interstitials in solution, precipitate particles, and strain. The significance of k is still unresolved. The experimental data suggest that

(over)

UNCLASSIFIED

Aerospace Corporation, El Segundo, California. YIELDING AND FLOW OF IRON, prepared by H. Conrad. 27 February 1963. [39] p. incl. illus. (Report TDR-169(3240-11)TN-2;SSD-TDR-63-27) (Contract AF 04(695)-169) Unclassified report

The significance of the parameters of the Hall-Petch equation for yielding and flow of iron and steel are discussed. The available experimental data suggest that σ^* represents the thermally-activated overcoming of the Peierls-Nabarro stress. The variations in σ^* with structure can be interpreted as changes in either dislocation density contributing to the deformation or the average distance the dislocations move per successful thermal fluctuation. Good agreement between experiment and theory is found for the contributions to σ_μ of interstitials in solution, precipitate particles, and strain. The significance of k is still unresolved. The experimental data suggest that

(over)

UNCLASSIFIED

Aerospace Corporation, El Segundo, California. YIELDING AND FLOW OF IRON, prepared by H. Conrad. 27 February 1963. [39] p. incl. illus. (Report TDR-169(3240-11)TN-2;SSD-TDR-63-27) (Contract AF 04(695)-169) Unclassified report

The significance of the parameters of the Hall-Petch equation for yielding and flow of iron and steel are discussed. The available experimental data suggest that σ^* represents the thermally-activated overcoming of the Peierls-Nabarro stress. The variations in σ^* with structure can be interpreted as changes in either dislocation density contributing to the deformation or the average distance the dislocations move per successful thermal fluctuation. Good agreement between experiment and theory is found for the contributions to σ_μ of interstitials in solution, precipitate particles, and strain. The significance of k is still unresolved. The experimental data suggest that

(over)

UNCLASSIFIED

Aerospace Corporation, El Segundo, California. YIELDING AND FLOW OF IRON, prepared by H. Conrad. 27 February 1963. [39] p. incl. illus. (Report TDR-169(3240-11)TN-2;SSD-TDR-63-27) (Contract AF 04(695)-169) Unclassified report

The significance of the parameters of the Hall-Petch equation for yielding and flow of iron and steel are discussed. The available experimental data suggest that σ^* represents the thermally-activated overcoming of the Peierls-Nabarro stress. The variations in σ^* with structure can be interpreted as changes in either dislocation density contributing to the deformation or the average distance the dislocations move per successful thermal fluctuation. Good agreement between experiment and theory is found for the contributions to σ_μ of interstitials in solution, precipitate particles, and strain. The significance of k is still unresolved. The experimental data suggest that

(over)

UNCLASSIFIED

the yield point in iron and steel is not due to the thermally-activated unlocking of dislocations from an interstitial atmosphere, but rather is associated with the decrease in dislocation velocity due to the sudden multiplication of dislocations by the double cross-slip mechanism. Stress-strain curves for mild steel calculated on the basis of this latter mechanism are in good agreement with the experimental curves.

UNCLASSIFIED

UNCLASSIFIED

the yield point in iron and steel is not due to the thermally-activated unlocking of dislocations from an interstitial atmosphere, but rather is associated with the decrease in dislocation velocity due to the sudden multiplication of dislocations by the double cross-slip mechanism. Stress-strain curves for mild steel calculated on the basis of this latter mechanism are in good agreement with the experimental curves.

UNCLASSIFIED

UNCLASSIFIED

the yield point in iron and steel is not due to the thermally-activated unlocking of dislocations from an interstitial atmosphere, but rather is associated with the decrease in dislocation velocity due to the sudden multiplication of dislocations by the double cross-slip mechanism. Stress-strain curves for mild steel calculated on the basis of this latter mechanism are in good agreement with the experimental curves.

UNCLASSIFIED

UNCLASSIFIED

the yield point in iron and steel is not due to the thermally-activated unlocking of dislocations from an interstitial atmosphere, but rather is associated with the decrease in dislocation velocity due to the sudden multiplication of dislocations by the double cross-slip mechanism. Stress-strain curves for mild steel calculated on the basis of this latter mechanism are in good agreement with the experimental curves.

UNCLASSIFIED

UNCLASSIFIED